Virology 501 (2017) 183–187

Contents lists available at ScienceDirect

Virology

journal homepage: www.elsevier.com/locate/yviro

MOPS and coxsackievirus B3 stability

Steven D. Carson[a,*], Susan Hafenstein[b], Hyunwook Lee[b]

[a] Department of Pathology and Microbiology University of Nebraska Medical Center, 986495 Nebraska Medical Center, Omaha, NE 68198-6495, USA
[b] Department of Medicine, The Pennsylvania State University College of Medicine, 500 University Drive, Hershey, PA 17033, USA

ARTICLE INFO

Keywords:
Coxsackievirus
Stability
MOPS
pH

ABSTRACT

Study of coxsackievirus B3 strain 28 (CVB3/28) stability using MOPS to improve buffering in the experimental medium revealed that MOPS (3-morpholinopropane-1-sulfonic acid) increased CVB3 stability and the effect was concentration dependent. Over the pH range 7.0–7.5, virus stability was affected by both pH and MOPS concentration. Computer-simulated molecular docking showed that MOPS can occupy the hydrophobic pocket in capsid protein VP1 where the sulfonic acid head group can form ionic and hydrogen bonds with Arg95 and Asn211 near the pocket opening. The effects of MOPS and hydrogen ion concentrations on the rate of virus decay were modeled by including corresponding parameters in a recent kinetic model. These results indicate that MOPS can directly associate with CVB3 and stabilize the virus, possibly by altering capsid conformational dynamics.

1. Introduction

Members of the *Picornaviridae* family, species *Human Enterovirus B*, group B coxsackieviruses are causative agents of myocarditis, pancreatitis, and other human diseases (Kim et al., 2001; Tam, 2006). These viruses have non-enveloped icosahedral 30 nm diameter capsids that enclose a positive-sense single-stranded RNA genome. The capsid is comprised of four viral proteins (VP1 to 4) that provide topological features that are important to the virus life cycle, including recognition of the coxsackievirus and adenovirus receptor (CAR) on host cells. The CAR binding site is localized to topological depressions, called “the canyon”, which surround each five-fold axis of icosahedral symmetry (He et al., 2001; Muckelbauer et al., 1995; Organtini et al., 2014). Similar to other enteroviruses, including poliovirus, and some human rhinoviruses, an opening in the canyon leads to a hydrophobic pocket in capsid protein VP1 that is occupied by a lipid moiety called “pocket factor” which is thought to confer stability to the capsid (Filman et al., 1989; Liu et al., 2015; Muckelbauer et al., 1995; Oliveira et al., 1993; Smyth et al., 1995). Replacement of the pocket factor with antiviral drugs (e.g. Pleconaril or WIN compounds) further stabilizes the capsid and prevents structural changes required for formation of the A-particle, a cell-entry intermediate, and subsequent uncoating of the genome (Lewis et al., 1998; Liu et al., 2015; Reisdorph et al., 2003; Schmidtke et al., 2005; Tsang et al., 2000). Virus stability is of particular interest considering that these capsid-stabilizing drugs inhibit infection, and viruses with different stabilities can have niche-specific reproductive advantages related to the density of the available cell surface receptor (Carson et al., 2011, 2016).

We have been investigating the effects of capsid mutations and the CAR on coxsackievirus B3 (CVB3; serotype 3 of 6) stability, tropism, and virulence (Carson et al., 2011; Carson et al., 2016; Organtini et al., 2014). Since this work has been done in cell culture, tissue culture medium and cell culture conditions comprise the environment most relevant to our interests. Enteroviruses are more stable below than above pH 7 (e.g., (Salo and Cliver, 1976; Wetz and Kucinski, 1991)) and Good's buffers have been used to help control pH in tissue culture for many years (Good et al., 1966). Experiments reported here using MOPS (3-morpholinopropane-1-sulfonic acid) to stabilize the pH indicated that it also stabilized CVB3, independent of its effect on pH, decreasing the CVB3 rate of decay at 37 °C. MOPS may contribute to CVB stability in a manner similar to pocket factors and pocket-binding antivirals that can occupy the hydrophobic pocket in capsid protein VP1, and consequently complicate studies of virus stability and dynamics.

2. Materials and methods

RDt3 cells (RD cells expressing truncated CAR (Cunningham et al., 2003)) and lab strain HeLa cells (Carson and Pirruccello, 2013) were maintained in Dulbecco's modified Eagle's medium with 10% fetal bovine serum in a 37 °C incubator with 6% CO_2. Five milliliters of 200 mM glutamine, 10 mL penicillin/streptomycin (10000 U/mL and 10 mg/mL, respectively) and 1.5 mL gentamicin (50 mg/mL), all from Gibco /Life Technologies, were added to each 1.1 l of DMEM-10%

* Corresponding author.
E-mail addresses: scarson@unmc.edu (S.D. Carson), shafenstein@hmc.psu.edu (S. Hafenstein), hyl5126@psu.edu (H. Lee).

http://dx.doi.org/10.1016/j.virol.2016.12.002
Received 7 September 2016; Received in revised form 30 November 2016; Accepted 2 December 2016
Available online 08 December 2016
0042-6822/

serum (the complete medium is referred to as DMEM-10). MOPS (Sigma-Aldrich) was added to the DMEM-10 to the final experimental concentration, and pH was adjusted to target values using 4 M NaOH. NaCl was added (50–200 mM) to separate samples of DMEM-10 used as controls for salt effects. Separate 4 mL aliquots of medium were placed in the incubator and used to determine the incubation pH at the end of each decay time course. Except at pH 7.4 (the pH of DMEM-10 in 6% CO_2) the experimental pH was different than the initial adjusted pH of the DMEM-10 with MOPS.

CVB3 strain 28 (CVB3/28) (Tracy et al., 2002; Tu et al., 1995) was propagated following transfection of a cloned infectious cDNA in HeLa cells. Virus stocks were prepared from frozen–thawed (three cycles) lysed monolayer cultures. Cell debris was removed by low-speed centrifugation and the supernatant was extracted with an equal volume of chloroform. Virus was partially purified by ultracentrifugation through 30% (w/v) sucrose, 1 mM $MgCl_2$, 0.1 M NaCl, and 0.02 M Tris/HCl (pH 7.5) into approximately 200 uL glycerol. Virus was suspended in 0.1 M NaCl and stored at −80 °C (Carson et al., 2011; Tu et al., 1995). Infectious virus titers were determined as 50% tissue culture infectious dose per mL (TCID50/mL) using RDt3 cells.

Virus stabilities were assessed in terms of the first-order rate constant for inactivation at 37 °C, as described previously (Organtini et al., 2014). Medium was incubated at 37 °C with 6% CO_2 overnight before adding virus. Starting virus concentrations in the different experiments were from 1×10^8 to 5×10^8 $TCID_{50}$/mL. Nine aliquots were taken from each sample over 70–80 h. The aliquots were placed into chilled tubes and stored at −80 °C until thawed for assay. Infectious virus was determined as the average of repeated $TCID_{50}$/mL analyses (duplicate; triplicate if the first two assays differed 5-fold or more). Samples were thawed and kept on ice until the assay dilutions were dispensed into the culture wells containing RDt3 cells. Two tubes containing medium and no virus were weighed at each time point to determine evaporation rates, and sample volumes for calculating virus titers were corrected accordingly. First-order rates for virus decay were determined from ln(V/Vo)=−k·t (k is the rate constant, h^{-1}, and t is elapsed time, h).

Molecular docking of the MOPS into the pocket area was simulated by using the program AutoDock Vina (Trott and Olson, 2010). The protein structure of VP1 was obtained from the crystal structure of CVB3 (PDB ID:1COV (Muckelbauer et al., 1995)) and the atomic model of MOPS was obtained from PubChem (CCDC Number 287618; (Chruszcz et al., 2005)). An exhaustive global search was performed and the best conformation of MOPS was chosen based on the free energy of the binding between the MOPS and the pocket area of VP1. The simulated model was analyzed and potential hydrogen bonds were identified in Chimera (Petterson et al., 2004).

Previous work showed that virus decay at 37 °C, in the absence of receptor, can be represented as

$$V \underset{K_{eq}}{\longleftrightarrow} U \underset{k}{\rightarrow} A \tag{1}$$

$$\frac{dA}{dt} = k \bullet U = k_{app} \bullet (V + U) \tag{2}$$

$$k_{app} = k \bullet \frac{K_{eq}}{K_{eq}+1} \tag{3}$$

V represents the closed conformation of the dynamic ("breathing") capsid, U the temperature-dependent open conformation, and A the A-particle (135 S particle). K_{eq} is the equilibrium constant for the conformational equilibrium, k is the first-order rate constant for transition from U to A, and k_{app} is the measured rate of decay (Carson, 2014; Organtini et al., 2014). Since enteroviruses are generally more stable at lower pH (Salo and Cliver, 1976; Wetz and Kucinski, 1991), a rational empirical solution can be proposed to include the effect of pH as a factor

$$\frac{K}{H^+ + K} \tag{4}$$

H^+ is the hydrogen ion concentration. K would normally be the acid dissociation constant of the relevant moiety (or average value for multiple moieties), but in the present context corresponds to the hydrogen ion concentration with half-maximal effect on measured virus stability. Since the effect of pH is implicitly included in the values of k and K_{eq} as a consequence of the "standard conditions" used in experiments to derive them (DMEM-10, 6% CO_2, 37 °C), to use these values and model the pH effect requires explicit inclusion of pH. The correction is provided by

$$\frac{K + H_0^+}{K} \tag{5}$$

H_0^+ represents the hydrogen ion concentration in the previous work (Carson, 2014; Organtini et al., 2014). The product of factor (4) multiplied by factor (5) equals one when H^+ equals H^+_0.

Kinetic model fitting and statistical calculations were done in PSI-Plot or Pro-Stat (Poly Software Intl., Pearl River, NY).

3. Results

DMEM-10 in the incubator with 6% CO_2 had a pH of 7.4, which was well-stabilized by addition of MOPS and adjustment to pH 7.4. But, the CVB3 first-order decay rate was diminished in the presence of MOPS (Fig. 1A). Comparing rates of virus decay with and without MOPS at pH 7.4 (Fig. 1A), H_o that the sample means are equal is rejected (t test; $p < 0.002$). Experiments with NaCl added to DMEM-10 from 50 mM to 200 mM showed that CVB3 was not stabilized by increased sodium from the NaOH used to adjust the pH. The CVB3 decay rates in the presence of added NaCl (n=4) were fully within the range of decay rates of CVB3 in DMEM-10 alone (n=4), and these data have been combined in the group with no added MOPS.

A plot of decay rate versus MOPS concentration showed that the stabilization effect was concentration-dependent (Fig. 1B). By simple linear regression of rate vs MOPS concentration for data obtained at pH 7.4 (Fig. 1B, symbols without dots), H_o slope=0 was rejected at $p < 0.001$ (p values remain significant at < 0.05 after Bonferroni's correction).

When medium plus MOPS was adjusted below pH 7.4, virus stability was observed to be affected by both pH and MOPS concentration. Rates of CVB3 decay in all samples over the pH range 7.0 to 7.5 (n=26, including the 17 at pH 7.4) are shown in Fig. 1B, C, and D. The virus was more stable at the lower pH, and the decay rate increased with increasing alkalinity.

We hypothesized that MOPS could stabilize CVB3 by occupying the hydrophobic pocket in VP1 and altering capsid dynamics. Simulated docking showed that MOPS does fit in the pocket (Fig. 2). In the binding model with the lowest calculated free energy, the morpholine ring sits near where the cis carbon-carbon kink in pocket factor (modelled as palmitate in 1COV) is located, while the sulfonate head group sits where the carboxylate group of pocket factor is located. The distances between oxygens of the sulfonate head group and nitrogens in the side chains of Arg95 and Asn211 were within 3.0–3.2 Å. In contrast, the distance between oxygens of the carboxyl group of the pocket factor and sidechains of Arg95 and Asn211 were 2.6–3.1 Å and 3.9–4.9 Å, respectively. Thus, it is likely that the sulfonate can form hydrogen bonds with both VP1 Arg95 and Asn211 near the pocket opening and a salt bridge with Arg95 is likely. The docking calculations show that MOPS is well-accommodated in the VP1 pocket, which might modify capsid dynamics as has been shown for other pocket-binding molecules (Reisdorph et al., 2003; Tsang et al., 2000).

If MOPS acts as a stabilizing pocket factor, Eq. (1) (see Materials and Methods) is modified to

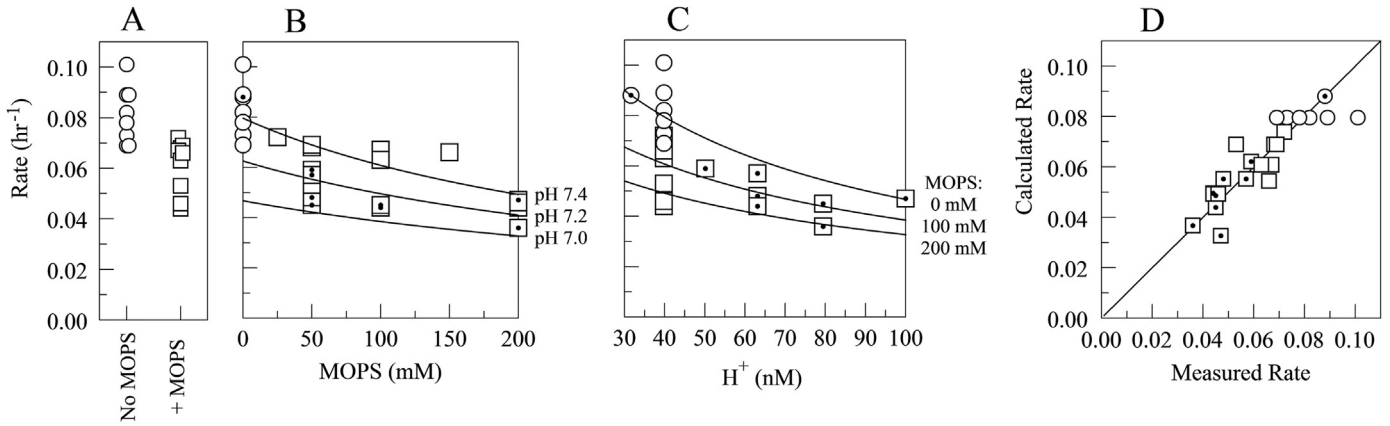

Fig. 1. CVB3/28 is more stable in the presence of MOPS and at lower pH. (A) Rates of CVB3 decay in samples with and without MOPS (25–200 mM) at pH 7.4. Virus in medium with MOPS was more stable than virus in medium without MOPS. Open circles correspond to samples at pH 7.4 with no MOPS; open squares correspond to samples with MOPS at pH 7.4. (B) The MOPS effect on CVB3 stability was dose dependent. Open symbols correspond to samples at pH 7.4; symbols containing a centered black dot represent samples at pH other than 7.4. The plotted lines were calculated with Eq. (8) at the pH values indicated. Note that the ordinate is scaled as total MOPS whereas Eq. (8) uses unprotonated MOPS calculated using the pH and pKa for MOPS at at 37 °C. (C) CVB3 stability increases with hydrogen ion concentration over the pH range of 7.5–7.0. Curves were calculated using Eq. (8) and the indicated concentrations of MOPS. (D) CVB3 decay rates calculated using Eq. (8) plotted against the measured rates. The line has slope equal to one.

$$VM \underset{K_d}{\leftrightarrow} M + V \underset{K_{eq}}{\longleftrightarrow} U \underset{k}{\rightarrow} A \tag{6}$$

M represents MOPS and K_d its dissociation equilibrium constant for binding a VP1 pocket within virus in the closed conformation. This model assumes that sites are independent and that MOPS does not bind the open conformation in which the pocket may be partially collapsed (Strauss et al., 2015; van Vlijmen and Karplus, 2005). The consequence of this scheme is that the concentration of V is reduced and Eq. (3) is modified to

$$k_{app} = k \bullet \frac{K_{eq}}{K_{eq} + 1 + \frac{M}{K_d}} \tag{7}$$

K_{eq} and k were previously determined, and their values, corrected for CAR dimerization, are 0.058 and 1.83/h, respectively (Carson, 2014). The pH effect cannot be rigorously modelled because the extent to which the pH effect is mediated through ionization of specific groups in the virus or protonation of the MOPS morpholine nitrogen is unknown.

The model including factors (4) and (5) for pH (see Material and Methods) is then

$$k_{app} = k \bullet \frac{K + H_0^+}{K + H^+} \bullet \frac{K_{eq}}{K_{eq} + 1 + \frac{M}{K_d}} \tag{8}$$

But, MOPS exists as protonated and unprotonated forms in equilibrium (pK_a=7.02 at 37 °C, per Sigma-Aldrich). Eq. (8) therefore should include two forms of "M" (the zwitterion and the anion) and two corresponding K_d values. Fitting the model by least-squares with both ionization states mathematically eliminated the protonated form of MOPS from consideration (($M_{protonated}/K_{d\_protonated}$) was vanishingly small). Consequently, in the most satisfying model the M and K_d in Eq. (8) represent the unprotonated MOPS. Eq. (8), with M and K_d representing unprotonated MOPS, was fit to the data by least squares and the best-fit parameters were solved as K_d=216 mM unprotonated MOPS, K=45.6 nM hydrogen ion (pK=7.34), and H^+_0=22.2 nM (pH=7.65). The lines plotted in Fig. 1B and C illustrate this solution using the best-fit parameters at several pH values and concentrations of MOPS. The coefficient of determination for the regression model was 0.768, indicating that the model accounts for nearly 77% of the variance in the measured CVB3 decay rate, as reflected in the plot of measured rates versus rates calculated with the model (Fig. 1 D). If H^+_0 is set to 39.8 nM (pH 7.4), an inter-experiment variability factor, f, is introduced to allow for experimental differences in k or K_{eq} in this work relative to previous work (Carson, 2014; Organtini et al., 2014). When k is replaced with f·k, f is solved as 0.79, Kd=216 mM, and K=45.6 nM. Or, if K_{eq} is replaced with f· K_{eq}, f is solved as 0.78, Kd=219 mM, and K=45.6 nM. The fits to the data are all the same as shown in Fig. 1 (B-D). That is, the solutions are equivalent irrespective of whether the model in Eq. (8) is allowed to vary H^+_0, k, or K_{eq} and the results for K_d and K are effectively unchanged.

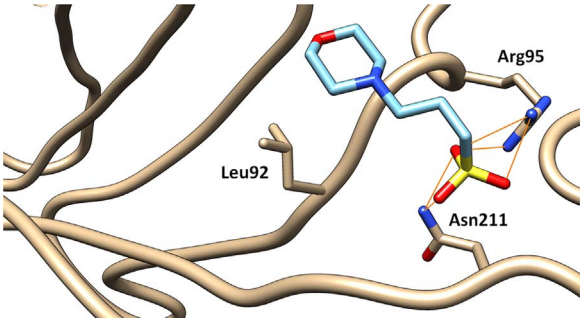

Fig. 2. Simulated docking of MOPS in the hydrophobic pocket within capsid protein VP1. The narrow lines illustrate potential hydrogen bonds between the oxygen atoms in the MOPS sulfonate group and the side chain nitrogens of asparagine at residue 211 and arginine at residue 95 of VP1. A salt bridge between the sulfonate and guanidino group is also likely. Leucine at residue 92 influences virus stability, is unusual among enteroviruses, and may limit the length of pocket factor that can be accommodated (Carson et al., 2016; Liu et al., 2015).

4. Discussion

Enteroviruses and rhinoviruses are dynamic particles that cycle between closed and open conformations, referred to as breathing (Lewis et al., 1998; Li et al., 1994). The temperature-dependent conformations appear to have different affinities for the receptors these viruses use to infect cells (Casasnovas and Springer, 1995; McDermott et al., 2000). The low-affinity closed conformation of these viruses predominates below physiological temperature and is stabilized at physiological temperature by molecules that bind the hydrophobic pocket in capsid protein VP1. Pocket factor, is modeled as palmitate in the coxsackievirus structure 1COV (Muckelbauer et al., 1995) and lipid-like molecules present in other enteroviruses and rhinoviruses have lengths ranging from eight to eighteen carbons (Ismail-Cassim et al., 1990; Liu et al., 2015; Plevka et al., 2012; Smyth and Martin, 2002). Pocket-binding antiviral drugs, such as WIN compounds, interfere with the capsid conformational dynamics, stabilizing the capsids to the extent that genome uncoating is inhibited (Lewis et al.,

1998; Liu et al., 2015; Reisdorph et al., 2003; Schmidtke et al., 2005; Tsang et al., 2000). The association between pocket occupancy and capsid stability led to the suggestion that host receptors used by the viruses displace pocket factor, thereby decreasing capsid stability and promoting genome uncoating. On the other hand, some picornaviruses naturally lack pocket factor yet remain viable, and a poliovirus complexed with modified receptor has been found to have lost its pocket factor without expanding to the A-particle (Strauss et al., 2015). So, it remains uncertain whether the receptors destabilize the viruses by displacing pocket factor, or whether the equilibrium between occupied and vacant VP1 pockets controls breathing and receptor destabilizes the capsid by shifting the conformational equilibrium to the open state. The kinetic model with independent sites and the structure of asymmetrically-destabilized coxsackievirus are consistent with the receptor stabilizing the open conformation that is available when the VP1 pocket is vacant (Carson, 2014; Lee et al., 2016; Organtini et al., 2014). Irrespective of which model is correct, it is evident that capsid stability and instability are integral to the virus life cycle, and environments that affect stability not only contribute to virus biology, but can complicate interpretation of in vitro studies.

MOPS has a stabilizing effect on CVB3 decay kinetics, as shown here. MOPS and MES can bind to various proteins (e.g., (Fitzgerald et al., 1998; Knochel et al., 1996; Long and Yang, 2009; Sigurdardottir et al., 2015)), and the weak interaction between MES and liver fatty acid binding protein is sufficient to alter protein dynamics (Long and Yang, 2009). Molecular modelling shows that MOPS is well-accommodated in the VP1 pocket, so it is reasonable to conclude that MOPS binds CVB3 and alters the capsid dynamics with a mechanism similar to that described for other pocket-binding molecules (Reisdorph et al., 2003; Tsang et al., 2000). Based on simulated docking, MES and HEPES are also accommodated in the pocket (not shown).

The model fit to the data is an extension of a model for dynamic virus where the open conformation is an intermediate to the A-particle (Carson, 2014). The modified kinetic equation, Eq. (8), includes terms for a competitive inhibitor (MOPS) that is mechanistically a heterotropic allosteric inhibitor (i.e., it inhibits the transition to the open intermediate conformation by stabilizing the closed conformation). The pH effect was empirically modelled with a factor where the hydrogen ion effect is half-maximal when it equals K. This is a necessary approach, pending greater knowledge, because the changes in pH affect virus, MOPS (the proportion of unprotonated MOPS is determined by pH), and other components in the experimental milieu, including any naturally occurring pocket factor(s) that might be present. Moreover, variations of the model suggested that the data were fit best when the unprotonated form of MOPS was considered to be the virus-stabilizing form. In this interpretation, MOPS and pH have antagonistic effects on virus stability: increasing pH destabilizes the virus but increases the concentration of the stabilizing form of MOPS.

Since the pH component of the model is empirical, the data covers a narrow range of pH values, and the calculated K_d exceeds the maximum concentration of MOPS tested, the K and K_d values, though physiologically reasonable, cannot accurately represent the true dissociation equilibrium constants. Nevertheless, the model should have reasonable predictive value for virus decay rate as a function of pH and MOPS concentration at least within the ranges studied, which are typical for such experiments. The results clearly show that MOPS and pH both affect CVB3 stability, and that MOPS (and probably other Good's buffers) should be avoided in studies that would be affected by increased CVB3 stability.

Acknowledgments

S.H. was funded in part by the Pennsylvania Department of Health CURE funds and by the Office of The Director, National Institutes of Health, under Award Numbers S10OD011986 and R01AI107121. SDC thanks Dr. Justin Stolen for helpful discussions regarding data analysis.

References

Carson, S.D., 2014. Kinetic models for receptor-catalyzed conversion of coxsackievirus B3 to A-particles. J. Virol. 88, 11568–11575.
Carson, S.D., Chapman, N.M., Hafenstein, S., Tracy, S., 2011. Variations of coxsackievirus B3 capsid primary structure, ligands, and stability are selected for in a coxsackievirus and adenovirus receptor-limited environment. J. Virol. 85, 3306–3314.
Carson, S.D., Pirruccello, S., 2013. HeLa cell heterogeneity and coxsackievirus B3 cytopathic effect: inplications for inter-laboratory reproducibility of results. J. Med. Virol. 85, 677–683.
Carson, S.D., Tracy, S., Kaczmarek, Z.G., Alhazmi, A., Chapman, N.M., 2016. Three capsid amino acids notably influence coxsackie B3 virus stability. J. Gen. Virol. 97, 60–68.
Casasnovas, J.M., Springer, T.A., 1995. Kinetics and thermodynamics of virus binding to receptor. Studies with rhinovirus, intercellular adhesion molecule-1 (ICAM-1), and surface plasmon resonance. J. Biol. Chem. 270, 13216–13224.
Chruszcz, M., Zheng, H., Cymborowski, M., Gawlicka-Chruszcz, A., Minor, W., 2005. 3-(morpholinium-1-yl)propanesulfonate. Acta Crystallogr. E Crystallogr. Commun. E61, o3190–o3191.
Cunningham, K.A., Chapman, N.M., Carson, S.D., 2003. Caspase-3 activation and ERK phosphorylation during CVB3 infection of cells: influence of the coxsackievirus and adenovirus receptor and engineered variants. Virus Res. 92, 179–186.
Filman, D.J., Syed, R., Chow, M., Macadam, A.J., Minor, P.D., Hogle, J.M., 1989. Structural factors that control conformational transitions and serotype specificity in type 3 poliovirus. EMBO J. 8, 1567–1579.
Fitzgerald, P.M., Wu, J.K., Toney, J.H., 1998. Unanticipated inhibition of the metallo-beta-lactamase from Bacteroides fragilis by 4-morpholineethanesulfonic acid (MES): a crystallographic study at 1.85-A resolution. Biochemistry 37, 6791–6800.
Good, N.E., Winget, G.D., Winter, W., Connolly, T.N., Izawa, S., Singh, R.M., 1966. Hydrogen ion buffers for biological research. Biochemistry 5, 467–477.
He, Y., Chipman, P.R., Howitt, J., Bator, C.M., Whitt, M.A., Baker, T.S., Kuhn, R.J., Anderson, C.W., Freimuth, P., Rossmann, M.G., 2001. Interaction of coxsackievirus B3 with the full length coxsackievirus-adenovirus receptor. Nat. Struct. Biol. 8, 874–878.
Ismail-Cassim, N., Chezzi, C., Newman, J.F., 1990. Inhibition of the uncoating of bovine enterovirus by short chain fatty acids. J. Gen. Virol. 71, 2283–2289.
Kim, K.S., Hufnagel, G., Chapman, N.M., Tracy, S., 2001. The group B coxsackieviruses and myocarditis. Rev. Med. Virol. 11, 355–368.
Knochel, T.R., Hennig, M., Merz, A., Darimont, B., Kirschner, K., Jansonius, J.N., 1996. The crystal structure of indole-3-glycerol phosphate synthase from the hyperthermophilic archaeon Sulfolobus solfataricus in three different crystal forms: effects of ionic strength. J. Mol. Biol. 262, 502–515.
Lee, H., Shingler, K.L., Organtini, L.J., Ashley, R.E., Makhov, A.M., Conway, J.F., Hafenstein, S., 2016. The novel asymmetric entry intermediate of a picornavirus captured with nanodiscs. Science Adv. 2, e1501929.
Lewis, J.K., Bothner, B., Smith, T.J., Siuzdak, G., 1998. Antiviral agent blocks breathing of the common cold virus. Proc. Natl. Acad. Sci. USA 95, 6774–6778.
Li, Q., Yafal, A.G., Lee, Y.M., Hogle, J., Chow, M., 1994. Poliovirus neutralization by antibodies to internal epitopes of VP4 and VP1 results from reversible exposure of these sequences at physiological temperature. J. Virol. 68, 3965–3970.
Liu, Y., Sheng, J., Fokine, A., Meng, G., Shin, W.H., Long, F., Kuhn, R.J., Kihara, D., Rossmann, M.G., 2015. Structure and inhibition of EV-D68, a virus that causes respiratory illness in children. Science 347, 71–74.
Long, D., Yang, D., 2009. Buffer interference with protein dynamics: a case study on human liver fatty acid binding protein. Biophys. J. 96, 1482–1488.
McDermott, B.M., Jr., Rux, A.H., Eisenberg, R.J., Cohen, G.H., Racaniello, V.R., 2000. Two distinct binding affinities of poliovirus for its cellular receptor. J. Biol. Chem. 275, 23089–23096.
Muckelbauer, J.K., Kremer, M., Minor, I., Tong, L., Zlotnick, A., Johnson, J.E., Rossmann, M.G., 1995. Structure determination of coxsackievirus B3 to 3.5 A resolution. Acta Crystallogr. D. Biol. Crystallogr. 51, 871–877.
Oliveira, M.A., Zhao, R., Lee, W.M., Kremer, M.J., Minor, I., Rueckert, R.R., Diana, G.D., Pevear, D.C., Dutko, F.J., McKinlay, M.A., et al., 1993. The structure of human rhinovirus 16. Structure 1, 51–68.
Organtini, L.J., Makhov, A.M., Conway, J.F., Hafenstein, S., Carson, S.D., 2014. Kinetic and structural analysis of coxsackievirus B3 receptor interactions and formation of the A-particle. J. Virol. 88, 5755–5765.
Petterson, E.F., Goddard, T.D., Huang, C.C., Couch, G.S., Greenblatt, D.M., Meng, E.C., Ferrin, T.E., 2004. UCSF Chimera- A visualization system for exploratory research and analysis. J. Comput. Chem. 25, 1605–1612.
Plevka, P., Perera, R., Cardosa, J., Kuhn, R.J., Rossmann, M.G., 2012. Crystal structure of human enterovirus 71. Science 336, 1274.
Reisdorph, N., Thomas, J.J., Katpally, U., Chase, E., Harris, K., Siuzdak, G., Smith, T.J., 2003. Human rhinovirus capsid dynamics is controlled by canyon flexibility. Virology 314, 34–44.
Salo, R.J., Cliver, D.O., 1976. Effect of acid pH, salts, and temperature on the infectivity and physical integrity of enteroviruses. Arch. Virol. 52, 269–282.
Schmidtke, M., Hammerschmidt, E., Schuler, S., Zell, R., Birch-Hirschfeld, E., Makarov, V.A., Riabova, O.B., Wutzler, P., 2005. Susceptibility of coxsackievirus B3 laboratory strains and clinical isolates to the capsid function inhibitor pleconaril: antiviral studies with virus chimeras demonstrate the crucial role of amino acid 1092 in treatment. J. Antimicrob. Chemother. 56, 648–656.
Sigurdardottir, A.G., Winter, A., Sobkowicz, A., Fragai, M., Chirgadze, D., Ascher, D.B., Blundell, T.L., Gherardi, E., 2015. Exploring the chemical space of the lysine-binding

pocket of the first kringle domain of hepatocyte growth factor/scatter factor (HGF/SF) yields a new class of inhibitors of HGF/SF-MET binding. Chem. Sci. 6, 6147–6157.
Smyth, M., Tate, J., Hoey, E., Lyons, C., Martin, S., Stuart, D., 1995. Implications for viral uncoating from the structure of bovine enterovirus. Nat. Struct. Biol. 2, 224–231.
Smyth, M.S., Martin, J.H., 2002. Picornavirus uncoating. Mol. Pathol. 55, 214–219.
Strauss, M., Filman, D.J., Belnap, D.M., Cheng, N., Noel, R.T., Hogle, J.M., 2015. Nectin-like interactions between poliovirus and its receptor trigger conformational changes associated with cell entry. J. Virol. 89, 4143–4157.
Tam, P.E., 2006. Coxsackievirus myocarditis: interplay between virus and host in the pathogenesis of heart disease. Viral Immunol. 19, 133–146.
Tracy, S., Drescher, K.M., Chapman, N.M., Kim, K.S., Carson, S.D., Pirruccello, S., Lane, P.H., Romero, J.R., Leser, J.S., 2002. Toward testing the hypothesis that group B coxsackieviruses (CVB) trigger insulin-dependent diabetes: inoculating nonobese diabetic mice with CVB markedly lowers diabetes incidence. J. Virol. 76, 12097–12111.
Trott, O., Olson, A.J., 2010. AutoDock Vina: improving the speed and accuracy of docking with a new scoring function, efficient optimization, and multithreading. J. Comput. Chem. 31, 455–461.
Tsang, S.K., Danthi, P., Chow, M., Hogle, J.M., 2000. Stabilization of poliovirus by capsid-binding antiviral drugs is due to entropic effects. J. Mol. Biol. 296, 335–340.
Tu, Z., Chapman, N.M., Hufnagel, G., Tracy, S., Romero, J.R., Barry, W.H., Zhao, L., Curry, K., Shapiro, B., 1995. The cardiovirulent phenotype of coxsackievirus B3 is determined at a single site in the 5' nontranslated region. J. Virol. 69, 4607–4618.
van Vlijmen, H.W., Karplus, M., 2005. Normal mode calculations of icosahedral viruses with full dihedral flexibility by use of molecular symmetry. J. Mol. Biol. 350, 528–542.
Wetz, K., Kucinski, T., 1991. Influence of different ionic and pH environments on structural alterations of poliovirus and their possible relation to virus uncoating. J. Gen. Virol. 72, 2541–2544.